Comparison of the Diagnostic Utility of Cardiac Magnetic Resonance Imaging, Computed Tomography, and Echocardiography in Assessment of Suspected Pulmonary Arterial Hypertension in Patients with Connective Tissue Disease

SMITHA RAJARAM, ANDREW JAMES SWIFT, DAVID CAPENER, CHARLES A. ELLIOT, ROBIN CONDLIFFE, CHRISTINE DAVIES, CATHERINE HILL, JUDITH HURDMAN, RACHAEL KIDLING, MOHAMMED AKIL, JIM M. WILD, and DAVID G. KIELY

ABSTRACT. ***Objective.*** Pulmonary arterial hypertension (PAH) is a life-threatening complication of connective tissue diseases (CTD). Our aim was to compare the diagnostic utility of noninvasive imaging modalities, i.e., magnetic resonance imaging (MRI), computed tomography (CT), and echocardiography, in evaluation of these patients.

Methods. In total, 81 consecutive patients with CTD and suspected PH underwent cardiac MRI, CT, and right heart catheterization (RHC) within 48 hours. Functional cardiac MRI variables [ventricle areas and ratios, delayed myocardial enhancement, position of the interventricular septum, right ventricular mass, ventricular mass index (VMI), and pulmonary artery distensibility] were all evaluated. The pulmonary artery size, pulmonary artery/aortic ratio (PA/Ao), left and right ventricular (RV) diameter ratio, RV wall thickness, and grade of tricuspid regurgitation were measured on CT. Tricuspid gradient (TG) and size of the RV were assessed using echocardiography.

Results. In our study of 81 patients with CTD, 55 had PAH, 22 had no PH, and 4 had PH owing to left heart disease. There was good correlation between mean pulmonary artery pressure (mPAP) and pulmonary vascular resistance (PVR) measured by RHC and VMI derived from MRI (mPAP, $r = 0.69$, $p < 0.001$; PVR, $r = 0.78$, $p < 0.001$) and systolic area ratio (mPAP, $r = 0.69$, $p < 0.001$; PVR, $r = 0.68$, $p < 0.001$) and TG derived from echocardiography (mPAP, $r = 0.84$, $p < 0.001$; PVR, $r = 0.76$, $p < 0.001$). In contrast, CT measures showed only moderate correlation. MRI and echocardiography each performed better as a diagnostic test for PAH than CT-derived measures: VMI ≥ 0.45 had a sensitivity of 85% and specificity 82%; and TG ≥ 40 mm Hg had a sensitivity of 86% and specificity 82%. Univariate Cox regression analysis showed the MRI measurements were better at predicting mortality. Patients with RV end diastolic volume < 135 ml had a better prognosis than those with a value > 135 ml, with a 1-year survival of 95% versus 66%, respectively.

Conclusion. In patients with CTD and suspected PAH, cardiac MRI and echocardiography have greater diagnostic utility than CT in the assessment of patients with suspected PAH, and MRI has prognostic value. (J Rheumatol First Release May 15 2012; doi:10.3899/jrheum.110987)

Key Indexing Terms:
PULMONARY ARTERIAL HYPERTENSION
CONNECTIVE TISSUE DISEASE
COMPUTED TOMOGRAPHY
SYSTEMIC SCLEROSIS
MAGNETIC RESONANCE IMAGING
SURVIVAL

From the Unit of Academic Radiology, University of Sheffield; Sheffield Pulmonary Vascular Disease Unit, Royal Hallamshire Hospital, Sheffield Teaching Hospitals, National Health Service (NHS) Foundation Trust; and Department of Radiology and Department of Rheumatology, Sheffield Teaching Hospitals Trust, Sheffield, UK.

S. Rajaram and D. Capener are supported by unrestricted research grants from Pfizer and Bayer, respectively. A.J. Swift, R. Condliffe, C. Davies, J.M. Wild, and D.G. Kiely receive funding from the National Institute for Health Research through the Biomedical Research Units funding scheme. J.M. Wild is also funded by the Engineering and Physical Sciences Research Council.

S. Rajaram, FRCR, Unit of Academic Radiology, University of Sheffield, Department of Radiology, Sheffield Teaching Hospitals Trust; A.J. Swift, BMedSci, FRCR; D. Capener, MSc, Unit of Academic Radiology, University of Sheffield; C.A. Elliot, MRCP; R. Condliffe, MRCP, MD; Sheffield Pulmonary Vascular Disease Unit, Royal Hallamshire Hospital, Sheffield Teaching Hospitals, NHS Foundation Trust; C. Davies, FRCR; C. Hill, FRCR, Department of Radiology, Sheffield Teaching Hospitals Trust; J. Hurdman, MRCP, Sheffield Pulmonary Vascular Disease Unit, Royal Hallamshire Hospital, Sheffield Teaching Hospitals, NHS Foundation Trust; R. Kidling, FRCP; M. Akil, FRCP, Department of Rheumatology, Sheffield Teaching Hospitals Trust; J.M. Wild, PhD, Unit of Academic Radiology, University of Sheffield; D.G. Kiely, FRCP, MD, Sheffield Pulmonary Vascular Disease Unit, Royal Hallamshire Hospital, Sheffield Teaching Hospitals, NHS Foundation Trust.

Address correspondence to Dr. S. Rajaram, Unit of Academic Radiology, University of Sheffield, Sheffield, UK. E-mail: s.rajaram@sheffield.ac.uk

Accepted for publication March 2, 2012.

Pulmonary arterial hypertension (PAH) is a serious complication of connective tissue disease (CTD) and is one of the leading causes of mortality[1]. The prevalence of CTD-associated PAH (CTD-PAH) is estimated to be as high as 13% based on right heart catheterization (RHC)[2]. This is most commonly seen in the setting of systemic sclerosis (SSc), whereas in patients with systemic lupus erythematosus the estimated prevalence is < 1%[3]. Patients with CTD-PAH generally have a poor outcome compared to those with idiopathic PAH[3,4,5]. Within this group, patients with PAH associated with SSc have the poorest prognosis.

Diagnostic tools capable of identifying the presence of PAH with a high degree of accuracy and identifying patients at increased risk of early mortality are essential in this patient population. Echocardiography is recommended as a screening test, with annual echocardiography recommended in patients with SSc and in other forms of CTD when patients have symptoms of breathlessness. However, estimates of pulmonary artery pressure (PAP) cannot always be made and echocardiography can both underestimate and overestimate PAP. RHC remains the "gold standard" to confirm a diagnosis of PH but this is an invasive investigation. In addition it gives only limited information on the cause of PH and gives no detail of the morphology of the cardiac chambers or the pulmonary vascular bed. A noninvasive test that may aid the clinician in risk stratification of patients with CTD who have a poor-quality echocardiogram or in whom the results are equivocal would be of value in diagnosing the presence of PH and aiding classification.

Patients with suspected CTD-PAH routinely undergo high-resolution chest computed tomography (HRCT) to diagnose the presence of interstitial lung disease (ILD) and often CT pulmonary angiography to exclude thromboembolic disease. Cardiac MRI is currently the standard method for morphological and quantitative assessment of cardiac function, and there is increasing interest in its use as a diagnostic tool in patients with suspected PH[6]. Studies have evaluated cardiac MRI and CT for prediction of the severity of PH associated with various etiologies[7,8,9,10], but very little has been reported on the role of cardiac MRI in patients with CTD and suspected PAH. Our aim was to compare the diagnostic usefulness of various MRI, CT, and echocardiographic measures with RHC in patients with CTD and suspected PH, and to evaluate the ability of these imaging modalities to assess severity of PAH and predict mortality.

MATERIALS AND METHODS

Study group. This was a retrospective study of 81 consecutive patients suspected of having CTD-PH and identified from a large cohort of patients referred to our center with suspected PH. The study was carried out in a nationally designated referral center for PH with a referral population of 15 million. Patients were referred to our center for further evaluation of clinical features suggesting PH or after implementation of a screening protocol using the combination of echocardiography, lung function testing, and assessment of symptoms of breathlessness. We recommend that screening be performed in patients with SSc on an annual basis in rheumatology centers referring to our center. From the screening program, patients underwent cardiac catheterization (1) if tricuspid gradient (TG) was ≥ 40 mm Hg; (2) if the TG was ≥ 30 mm Hg but < 40 mm Hg with DLCO < 50%; or (3) in the presence of symptoms of unexplained progressive breathlessness regardless of the results of the echocardiogram[11]. The diagnosis of CTD was made according to standard criteria and in most cases this was by the referring physician[12,13,14]. Patients in the study were required to have had CT, MRI, and RHC performed within 48 hours. For comparison with echocardiography this had to be performed at our center within 3 months of RHC. Local research ethics committee approval was obtained for retrospective analysis of imaging techniques. All the CT and MRI scans were reviewed by 2 chest radiologists (SR, AS) blinded to RHC hemodynamics.

The study included patients from January 2008 to March 2010 with a median followup of 24 months. The census date for mortality was March 31, 2011. Patients were treated according to UK national guidelines and prescription of therapies was in accord with the UK national commissioning policy.

Echocardiography protocol. Echocardiography was performed using a Powervision 8000 instrument (Toshiba, Tokyo, Japan). Right ventricle size and TG were measured using the maximum velocity of tricuspid regurgitation and the simplified Bernoulli equation. The median time interval between echocardiogram and RHC was 34 days (interquartile range 3 to 59 days). In 9 patients the echocardiogram data were not available.

CT protocol. CT pulmonary angiography was performed on a 64-slice multidetector CT scanner (Light-Speed, General Electric Medical Systems, Milwaukee, WI, USA). The following measures were used: automated dose reduction 100 mA, 120 kV, 1 pitch, rotation time 0.5 s, 0.625-mm collimation, field of view (FOV) 400 × 400 mm; 100 ml intravenous contrast agent (Ultravist 300; Bayer Schering, Berlin, Germany) was administered at a rate of 5 ml/s. From the contrast-enhanced acquisition, HRCT images were reconstructed for every 10 mm using a high spatial resolution filter.

CT image analysis. The following CT variables were measured: widest short axis diameter of the main pulmonary artery (PA) and the corresponding transverse diameter of the ascending aorta. The right and left PA diameter were also noted[15]. The maximum short axis distance of the right and left ventricle and right ventricle wall thickness were measured in an axial plane as described[16]. The severity of reflux of contrast into the inferior vena cava (IVC) or hepatic veins was graded as 0 = no reflux into IVC; 1 = trace of reflux into IVC only; 2 = reflux into IVC but not hepatic veins; 3 = reflux into IVC and proximal hepatic veins; 4 = reflux into IVC and distal hepatic veins[17]. The presence or absence of pericardial effusion was also assessed on CT. HRCT images were graded for presence or absence of ILD using a scoring system described by Bezante, *et al*[18].

MRI protocol. MRI was performed on a 1.5-T whole-body scanner, the GE HDx (GE Healthcare). The following measures were used for 4-chamber and short-axis cine images: cardiac gated multislice balanced steady-state free-precession sequence, 20 frames per cardiac cycle, slice thickness 5 mm, FOV 48 × 43.2, matrix 256 × 256, BW 125 KHz/pixel, TR 3.7 ms, and TE 1.6 ms. For delayed myocardial enhancement (DME), a short-axis inversion recovery sequence was performed at a single timepoint 10–12 min after intravenous injection of 0.05 ml/kg Gadovist (Bayer, Berlin, Germany). The phase-contrast sequence was performed orthogonal to the pulmonary artery trunk using an electrocardiogram-gated sequence with TR 5.6 ms, TE 2.7 ms, slice thickness 10 mm, FOV 48 × 28.8, and matrix 256 × 128.

MRI analysis. The contours of the right ventricle (RV) and left ventricle (LV) were delineated manually by a blinded observer in the short-axis stack images and processed using GE software. The RV end diastolic volume (RVEDV), RV end systolic volume (RVESV), RV ejection fraction, stroke volume, and cardiac output were then calculated. The systolic and diastolic areas of the RV and LV chambers were measured on the mid-4-chamber view and a ratio was derived. The RV end diastolic mass (RVEDM), left ventricular end diastolic mass (LVEDM) and the ventricular mass index as the ratio of RVEDM/LVEDM (VMI) were calculated from the end diastolic short-axis stack of images[19]. The RV longitudinal and transverse motion was quantified on the mid-4-chamber cardiac view by means of the tricuspid annular systolic

excursion (TAPSE) and septum-to-free wall distance, respectively, according to the method described by Kind, *et al*[20] (Figures 1 and 2). From the mid-4-chamber image the RV relative area change (RV area in end diastole – RV area in end systole/RV area in end diastole × 100) and systolic and diastolic RV/LV area ratios were measured (Figure 3). Phase-contrast MRI were processed using specialized software. The contours of the main PA were traced simultaneously on magnitude and velocity-map images and peak velocity, PA blood flow, and PA distensibility were calculated[21]. The motion of the interventricular septum was visually analyzed on short-axis and 4-chamber views for presence or absence of paradoxical septal movement. The presence or absence of myocardial delayed enhancement at the interventricular septum insertion points was also noted (Figure 4).

Right heart catheterization. RHC was performed through the internal jugular vein using a 7 French Swan-Ganz catheter by one of 3 PH consultants (DGK, CAE, RC). The form of PH was classified according to standard criteria[22] and required at RHC a mean pulmonary artery pressure (mPAP) ≥ 25 mm Hg to establish a diagnosis of PH. Patients with PAH were required to have mPAP ≥ 25 mm Hg and pulmonary wedge pressure ≤ 15 mm Hg.

Statistical analysis. The statistical analysis was performed with SPSS version 16.0 (SPSS, Chicago, IL, USA). To compare CT and MRI measurements between patients with PH and no-PH subjects, independent t tests and chi-square tests were used as appropriate. Pearson's test was used to determine correlations between imaging and RHC measures. Diagnostic strength, for identification of patients with PAH, was assessed using receiver-operated characteristic (ROC) curve analysis. Survival curves were derived using the Kaplan-Meier method and were compared using a log-rank test. Median values were used to separate continuous variables into 2 groups. Univariate Cox regression analysis was used to calculate the hazard ratio and CI for the following predictors: age, mean right atrial pressure, mixed venous oxygen saturation, cardiac index, mPAP, pulmonary vascular resistance (PVR), RVEDM, RVEDV, pulmonary artery to aortic ratio (PA/Ao), and RV wall thickness. A p value of < 0.05 was considered statistically significant for all analysis.

RESULTS

Demographic data. In total, 81 patients with CTD were identified, of whom 55 had PAH and 4 had PH owing to left heart disease. Twenty-two patients with CTD had "no PH." Phase-contrast MRI was performed in 51 patients and the ventricular mass was available for 62 patients. The study profile is out-

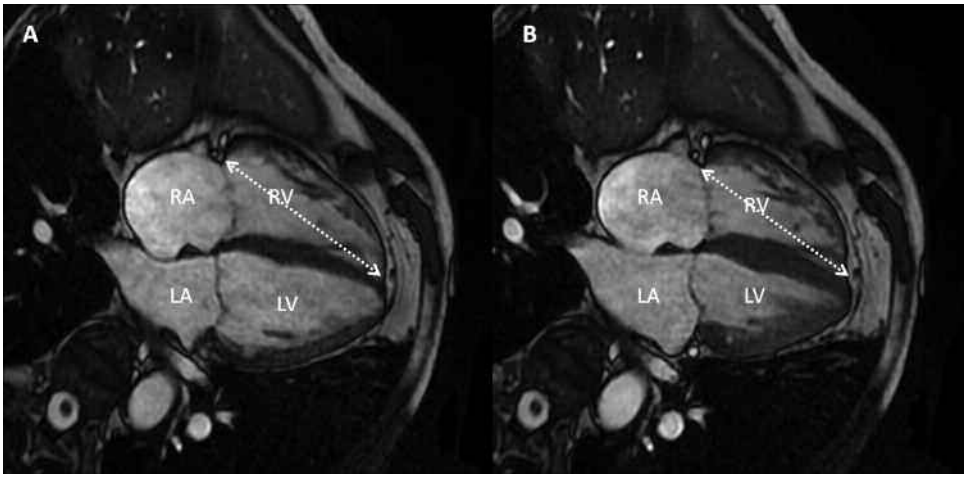

Figure 1. Tricuspid annular systolic excursion, a measure of longitudinal shortening of the right ventricle (RV), is the distance from base of the tricuspid annulus to the ventricular apex in the mid-4-chamber view at end systole (A) and end diastole (B). LV: left ventricle; RA: right atrium; LA: left atrium.

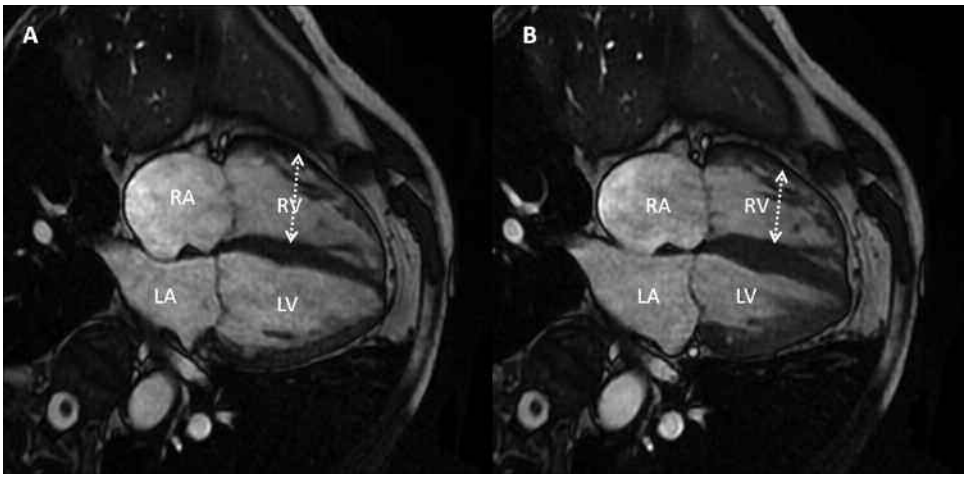

Figure 2. Septal-to-free wall distance, transverse distance between the interventricular septum and the free wall of the right ventricle (RV), is measured in the mid-4-chamber view at end systole (A) and end diastole (B). LV: left ventricle; RA: right atrium; LA: left atrium.

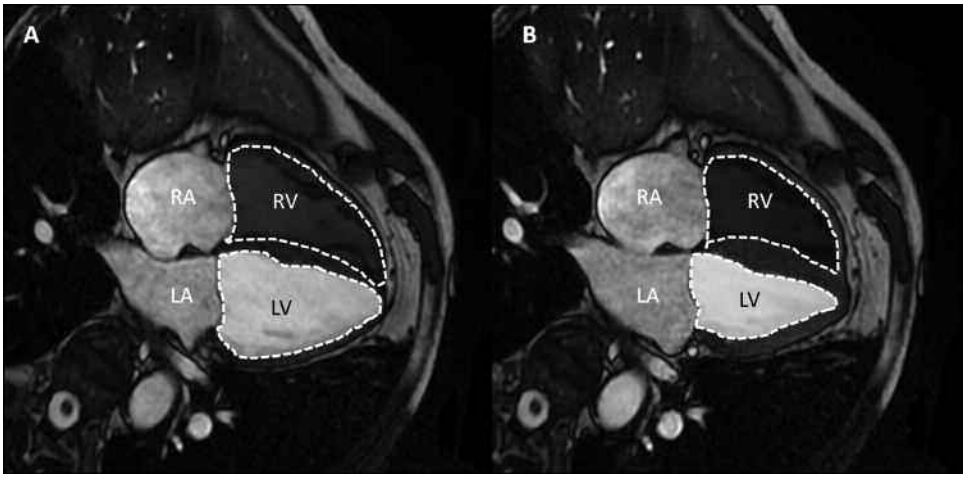

Figure 3. Right ventricle (RV) relative area change was measured by manually tracking the contours of the RV and left ventricle (LV) in the mid-chamber view at end systole (A) and end diastole (B). RA: right atrium; LA: left atrium.

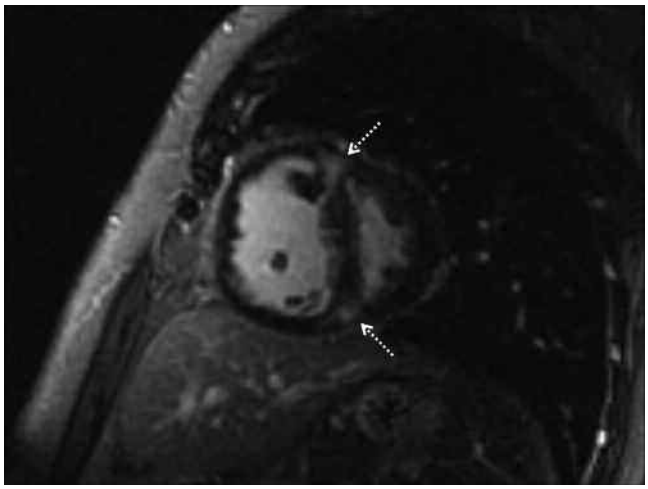

Figure 4. Example of short-axis stack imaging showing presence of delayed myocardial enhancement at the insertion points (arrows) of the interventricular septum.

lined in Figure 5 and patients' demographic details are summarized in Table 1.

Correlation of MRI, CT, and echocardiography findings with hemodynamic data. Table 2 summarizes the correlations between MRI measurements and mPAP and PVR derived from RHC. Good correlation was found between mPAP and PVR and VMI, RVEDM, and systolic and diastolic RV/LV area ratio; and a moderate correlation was found with TAPSE, PA distensibility, and right ventricle relative area change. The PA average blood flow measured from phase-contrast MRI showed a moderate correlation with cardiac output derived from RHC ($r = 0.59$, $p < 0.001$) but not with mPAP or PVR. For variables measured from CT scans, PA size, PA/Ao ratio, RV wall thickness, RV/LV ratio, and graded hepatic vein reflux showed only moderate correlation with the mPAP and PVR. The results of the CT and TG findings are summarized in Table 3. TG from echocardiography correlated strongly with mPAP and PVR measured at RHC (mPAP, $r = 0.84$, $p < 0.001$; and PVR, $r = 0.76$, $p < 0.001$).

Diagnostic value of MRI, CT, and echocardiography to identify PAH in the at-risk population. The performance of the MRI and CT scans and different thresholds of TG are outlined in Tables 4, 5, and 6. VMI was the best performing MRI measure, with a cutoff value ≥ 0.45 determined by ROC analysis [area under the curve (AUC) = 0.87], having a sensitivity of 85%, specificity of 82%, and likelihood ratio of 4.5. PA distensibility with the cutoff point ≤ 15 (AUC = 0.85) had a sensitivity of 80%, specificity of 78%, and likelihood ratio of 3.6. Of the CT measures evaluated, presence of PA/Ao ratio ≥ 1 (AUC = 0.71) had a low sensitivity of 59%, specificity of 73%, and likelihood ratio of 2.2. RV wall thickness ≥ 3.5 mm as determined by ROC analysis (AUC = 0.73) showed a sensitivity of 65%, specificity of 67%, and likelihood ratio of 1.9. Although the presence of pericardial effusion had 100% specificity, the sensitivity was poor (23%), as this was present in only 12 patients. TG performed strongly as a diagnostic test for the group (AUC = 0.87). The strongest TG threshold for diagnosing PH was 40 mm Hg and at this cutoff point the sensitivity was 86%, specificity was 82%, and likelihood ratio was 4.6 for diagnosing PH.

Survival analysis. The mean followup period was 24 months and there were 10 deaths during the study period. Univariate Cox regression analysis demonstrated that mean right arterial pressure, mixed venous oxygen saturation, RVEDV, RVESV, VMI, and RVEDM predicted mortality in PAH (Table 7). Kaplan-Meier survival curves showed patients with RVEDV < 135 ml had significantly better survival than those with RVEDV > 135 ml (log-rank test, $p = 0.024$). The Kaplan-Meier survival curve for RVEDV is shown in Figure 6. In our group of patients, the Kaplan-Meier survival curve for VMI using a median value of 0.75 also predicted mortality with a p value of 0.04 (Figure 7). A multivariable analysis was not performed because of the low number of deaths.

DISCUSSION

We compared the diagnostic utility of MRI with that of CT

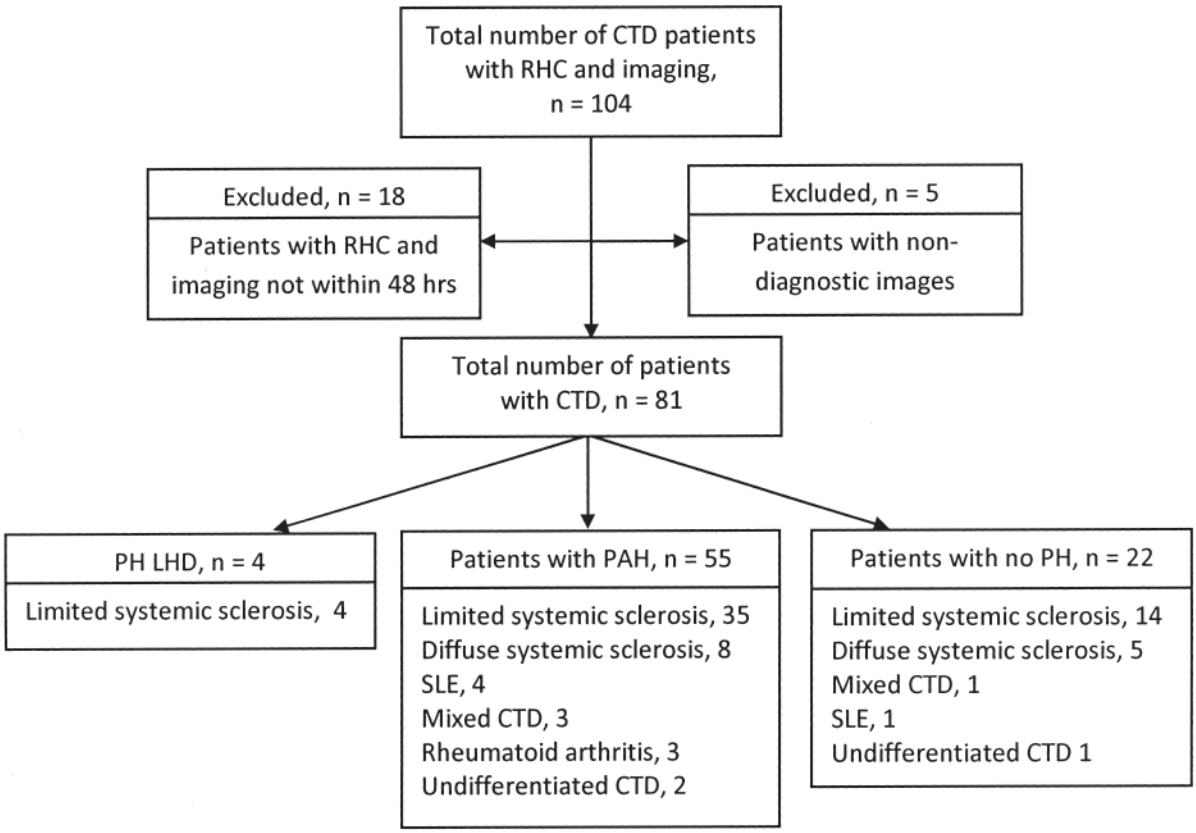

Figure 5. The patient classification process. CTD: connective tissue disease; RHC: right heart catheterization; PAH: pulmonary arterial hypertension; SLE: systemic lupus erythematosus; LHD: left heart disease.

Table 1. Patient demographics and right heart catheter data. Data are mean (SD) unless otherwise indicated.

Characteristic	Whole Group, n = 81	No PH, n = 22	PAH, n = 55	p
Age, yrs	62 (14)	59 (16)	64 (17)	0.47
Female, %	85	85	85	0.90
WHO II/III/IV, %	25:63:9	40:55:0	20:66:13	< 0.001
FVC, % predicted	85 (22)	91 (15)	82 (24)	0.11
TLCO, % predicted	47 (19)	67 (21)	40 (12)	< 0.001
mRAP, mm Hg	8 (5)	6 (3)	9 (5)	0.007
mPAP, mm Hg	35 (15)	19 (3)	40 (14)	< 0.001
PCWP, mm Hg	9 (4)	8 (3)	8 (3)	0.61
Cardiac index, l × min × m^2	3.3 (0.8)	3.7 (0.8)	3.2 (0.7)	0.004
PVR, dyn × s × cm^{-5}*	417 (393)	112 (46)	524 (404)	< 0.001
mVO_2, %	69 (8)	73 (7)	67 (8)	0.008

FVC: forced vital capacity; TLCO: gas transfer; mRAP: mean right atrial pressure; mPAP: mean pulmonary artery pressure; PVR: pulmonary vascular resistance; mVO_2: mixed venous oxygen saturation (n = 4 patients with LHD are included within the whole group); WHO: World Health Organization class; PCWP: pulmonary capillary wedge pressure; PAH: pulmonary arterial hypertension.

and selected echocardiographic measures, for the first time, in a large unselected group of patients with CTD and suspected PAH. We have demonstrated that both MRI and echocardiographic indices have a good correlation with mPAP and PVR at the time of RHC and performed well in predicting the presence of PAH in a high-risk population. In addition, measures of volume and mass derived from MRI predicted outcome. In contrast, CT indices correlated only moderately with invasive measures of pulmonary hemodynamics and had poorer diagnostic utility for PAH.

Several studies have investigated the role of echocardiography in the assessment of PH and have shown strong correlation with mPAP and PVR at RHC, and our results are in agreement with previous reports[23,24,25,26]. Echocardiography

Table 2. Correlations of cardiac MRI measurements with mPAP and PVR in the study group (n = 81).

Measurement	mPAP		PVR	
	r	p	r	p
Right ventricular mass, g/cm^3, n = 62	0.70	< 0.001	0.60	< 0.001
VMI, n = 62	0.69	< 0.001	0.78	< 0.001
Systolic RV/LV area ratio	0.69	< 0.001	0.68	< 0.001
Diastolic RV/LV area ratio	0.64	< 0.001	0.64	< 0.001
Pulmonary artery distensibility, %, n = 51	–0.58	0.0011	–0.54	0.0012
RVRAC, %	–0.53	< 0.001	–0.56	< 0.001
TAPSE, cm	–0.55	< 0.001	–0.58	< 0.001
SFD, cm	–0.39	0.0019	–0.44	< 0.001
RVEF, ml	–0.44	< 0.001	0.50	< 0.001
RVESV, ml	0.40	< 0.001	0.43	< 0.001
RVEDV, ml	0.24	0.09	0.20	0.12
RVSV, ml	–0.37	0.0026	–0.41	< 0.001
Average pulmonary blood flow, n = 51	–0.25	0.129	0.39	0.014

RVEDV: right ventricle end diastolic volume; RVESV: right ventricle end systolic volume; RVSV: right ventricle stroke volume; RVEF: right ventricle ejection fraction; TAPSE: transverse annular systolic excursion; SFD: septal-free wall distance; RVRAC: right ventricle relative area change; VMI: ventricular mass index.

Table 3. Correlations of computed tomography (CT) and echocardiography measures with mPAP and PVR.

Measurement	mPAP		PVR	
	r	p	r	p
CT				
Right ventricle wall thickness	0.47	< 0.001	0.35	0.007
Pulmonary artery size	0.37	0.003	0.28	0.03
PA/Ao ratio	0.43	< 0.001	0.36	0.004
RV/LV ratio	0.40	0.005	0.35	0.015
Hepatic vein reflux	0.53	0.001	0.58	0.001
Echocardiography				
Tricuspid gradient	0.84	< 0.001	0.76	< 0.001

mPAP: mean pulmonary artery pressure; PVR: pulmonary vascular resistance; RV/LV ratio: right ventricle/left ventricle transverse distance ratio; PA/Ao: pulmonary artery/aorta ratio.

is established in routine clinical practice for screening for PAH in SSc. The TG calculated from the peak tricuspid velocity is the most commonly used measure, with a TG ≥ 40 mm Hg having a good positive predictive value for the identification of PAH, which we have confirmed. However, there is no threshold that can confidently exclude the presence of PAH in symptomatic patients and this has resulted in interest in other diagnostic tests. Although cost-effective and readily available, echocardiography is operator-dependent and in 1 study, adequate estimation of the TG was not possible in roughly one-third of SSc patients with suspected PAH[27]. MRI is noninvasive and does not involve ionizing radiation, and importantly it allows detailed analysis of both structural and functional evidence, and in contrast to the TG measured by echocardiography these can be accurately quantified in the vast majority of patients. The utility of cardiac MRI in patients with sus-

Table 4. Diagnostic performance of MRI measurements for identification of pulmonary artery hypertension.

Variables	Sensitivity/ Specificity	PPV/NPV	LR	ROC AUC
Pulmonary artery distensibility ≤ 15	80/78	90/59	3.60	0.85
Right ventricle mass ≥ 30	72/80	91/50	3.57	0.84
VMI ≥ 0.45	85/82	92/69	4.5	0.87
RVRAC ≤ 36%	69/75	89/47	2.76	0.70
Systolic RV/LV area ratio < 1 vs ≥ 1	67/75	88/45	2.70	0.78
Diastolic RV/LV area ratio < 1 vs ≥ 1	60/75	87/40	2.40	0.73
TAPSE ≤ 2 cm	67/65	83/45	1.9	0.70
SFD ≤ 1	70/60	81/45	1.73	0.67
Delayed myocardial enhancement	74/82	89/63	4.09	—
Paradoxical septal movement	23/100	100/35	—	—
PA/Ao ratio ≥ 1	56/75	87/43	2.2	0.73
Average pulmonary blood flow ≥ 3.5	34/62	65/31	0.86	0.40

VMI: ventricular mass index; PPV: positive predictive value; NPV: negative predictive value; LR: likelihood ratio; ROC AUC: receiver-operator characteristics area under the curve; TAPSE: transverse annular systolic excursion; SFD: septal-free wall distance; RVRAC: right ventricle area change; PA/Ao: pulmonary artery/aorta ratio.

Table 5. Diagnostic performance of computed tomography measurements for identification of pulmonary artery hypertension.

Variables	Sensitivity/ Specificity	PPV/NPV	LR	ROC AUC
Pulmonary artery size ≥ 2.9	59/73	87/37	2.1	0.71
PA/Ao ratio ≥ 1	54/74	87/40	2.2	0.73
RV/LV ratio	55/53	76/30	1.2	0.54
Right ventricle wall thickness ≥ 3.5 mm	65/67	88/35	1.9	0.74
Hepatic vein reflux, present/absent	41/85	89/35	2.7	0.73

PPV: positive predictive value; NPV: negative predictive value; LR: likelihood ratio; ROC AUC: receiver-operator characteristics area under the curve; RV/LV ratio: right ventricle/left ventricle transverse distance ratio; PA/Ao: pulmonary artery/aorta ratio.

Table 6. Diagnostic performance of echocardiogram measurements for identification of pulmonary artery hypertension.

Variables	Sensitivity/ Specificity	PPV/NPV	LR	ROC AUC
Right ventricle size, normal/dilated	49/84	89/37	3.1	0.65
Tricuspid gradient threshold, mm Hg				
< 30 vs ≥ 30	95/43	79/82	1.67	
< 40 vs ≥ 40	86/82	91/73	4.62	0.87
< 50 vs ≥ 50	71/95	97/59	15.04	
< 60 vs ≥ 60	53/100	100/48	—	

PPV: positive predictive value; NPV: negative predictive value; LR: likelihood ratio; ROC AUC: receiver-operator characteristics area under the curve.

Table 7. Univariate predictors of mortality in patients with connective tissue disease pulmonary artery hypertension.

Variables	Hazard Ratio (95% CI)	p
Age, yrs	1.00 (0.95–1.05)	0.93
mRAP, mm Hg	1.2 (1.06–1.35)	0.003
mPAP, mm Hg	1.01 (0.96–1.06)	0.009
mVO_2, %	0.91 (0.84–0.98)	0.02
Cardiac index, $l/min^{-1}/m^{-2}$	0.59 (0.21–1.68)	0.328
PVR, $dyne/s/cm^{-5}$	1.00 (0.99–1.00)	0.307
RVSV, $ml/mm\ Hg^{-1}$	1.01 (0.98–1.04)	0.186
RVEF	0.99 (1.05–1.03)	0.923
RVEDV, ml	1.02 (1.01–1.03)	0.002
RVEDM, g/cm^3	1.03 (1.00–1.06)	0.040
VMI	5.56 (1.50–35.5)	0.013
Pulmonary artery distensibility, %	0.87 (0.64–1.18)	0.388
Tricuspid gradient	1.32 (0.33–5.30)	0.68

RVEF: right ventricle ejection fraction; RVEDV: right ventricle end diastolic volume; RVESV: right ventricle end systolic volume; mRAP: mean right arterial pressure; mPAP: mean pulmonary artery pressure; PVR: pulmonary vascular resistance; mVO_2: mixed venous saturation; RVEDM: right ventricular end diastolic volume; VMI: ventricular mass index.

pected CTD-PAH is underreported and has been limited to patients with SSc and PAH[18,26,28]. To our knowledge, our study is the first to analyze several quantitative MRI measures in a subgroup of patients with CTD and suspected PAH in comparison to gold standard RHC.

In PAH, a proliferative vasculopathy results in an increase in mPAP and PVR, leading to remodeling and compensatory hypertrophy of the RV. As the afterload continues to increase, RV dilatation and failure ensue[29]. Consequently, there has been interest in measures that are likely to reveal the remodeling process, such as RV mass and fluid overload as indicated by change in chamber volume. In our cohort, RV mass showed the best correlation with mPAP (RVEDM, r = 0.70; VMI, r = 0.68); this is not surprising because RV mass partially reflects the effect of RV afterload[29]. We and others have previously shown that VMI can predict disease severity in patients with PAH[19,30]; however, acquisition and post-processing for RV mass assessment is a time-consuming process. In our study we also demonstrated that simpler and quicker measurements such as RV/LV systolic area ratio also show good correlation with the catheter hemodynamics (mPAP, r = 0.68; PVR, r = 0.69). Indeed, as a diagnostic tool, PA distensibility measured from phase-contrast MRI was equally reliable in diagnosing PAH as VMI when the estimated value was ≤ 15, and this measurement can be performed rapidly. A simple approach to quantify systolic RV function has been to measure RV wall motion. Tricuspid annular plane systolic excursion (TAPSE) quantifies the longitudinal systolic function of the RV. Septum-to-free wall distance (SFD) is a measure of the transverse movement of the RV free wall and takes into consideration the position of the interventricular septum. Both these measures have previously been applied in MRI in patients with idiopathic PAH[20,31], and our results showed a

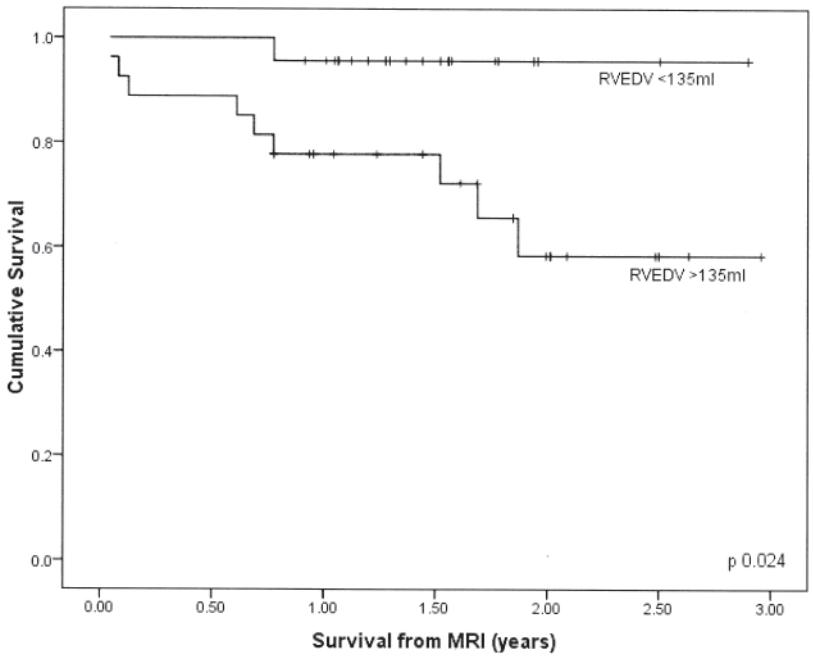

Figure 6. Kaplan-Meier survival curve for patients with connective tissue disease-associated pulmonary arterial hypertension based on right ventricle end diastolic volume (RVEDV). MRI: magnetic resonance imaging.

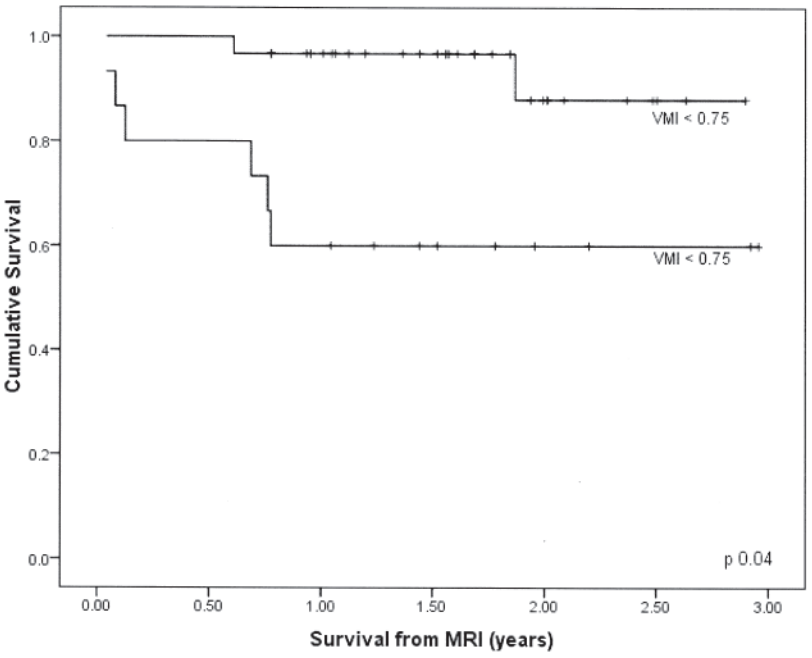

Figure 7. Kaplan-Meier survival curve for patients with connective tissue disease-associated pulmonary arterial hypertension based on ventricular mass index (VMI; n = 48).

better relationship of TAPSE with mPAP compared to SFD. Primary myocardial involvement has been reported in SSc and established myocardial involvement characteristically results in myocardial fibrosis[32]. On contrast-enhanced delayed MRI, scarring or fibrosis appears as an area of high signal intensity and characteristically occurs at the insertion points of the interventricular septum in patients with PAH[33]. Tzelepis, *et al* analyzed 36 patients with SSc and found 66% had DME[34]. The DME was characteristically mid-wall of the left ventricle; however, a small number of patients also had DME at the interventricular septum insertion points in the absence of PH as assessed on echocardiography. Our study

examined the prevalence of DME in patients with suspected PAH; interestingly, 4 patients with SSc had DME in the absence of PAH based on RHC. The process of "primary" myocardial involvement in SSc may account for this finding in our patients without PAH[35].

The development of PAH in patients with CTD is known to have a major effect on survival, and patients in this group have poorer prognosis compared to other forms of PAH[3,4,36]. VMI was noted to predict outcome in a selected group of patients with SSc-associated PAH[19]. In patients with PAH, Gan, *et al* found that PA distensibility, which is thought to reflect the stiffness of the pulmonary artery, was a strong predictor of mortality when measured noninvasively[37]. Van Wolferen, *et al* found that low stroke volume, RV end diastolic volume index, and impaired left ventricular filling independently predicted mortality in patients with PAH[29]. We have shown that these findings are broadly applicable in patients with CTD-PAH and have demonstrated the ability of MRI measurements of RV volume and VMI to identify patients with better outcome.

The widespread availability of CT has resulted in interest in using this in addition to echocardiography to improve diagnostic accuracy[23]. Chest CT is an important and established modality to investigate breathless patients with CTD and can provide useful morphological information. HRCT in particular can identify even subtle parenchymal lung involvement. In a recent study, we demonstrated moderate correlation between RV/LV ratio measured by CT and reflux of contrast into hepatic veins and pulmonary hemodynamics[23]. However, as individual measurements, the role of morphological CT data appears to be limited as a prognostic and diagnostic tool. PA measurement, one of the features routinely assessed on CT in suspected PH, is an unreliable predictor of the presence of PH in patients with ILD[38]. The extent of contrast reflux into the IVC and hepatic veins mirrors the regurgitant volume[39], and significant correlations between hepatic vein reflux and mPAP and PVR have been observed[23]; similar results were seen in our study. This sign, however, may not be very specific because a Valsalva maneuver during breath-hold will elevate right atrial pressure and can theoretically lead to contrast reflux. RV hypertrophy is common in the patients with PH. Revel, *et al* reported good agreement between RV wall thickness and mPAP in a cardiac-gated CT study in patients with PH[40]. We have reproduced a similar correlation in a subgroup of patients with CTD using noncardiac-gated CT. Our study, however, does establish that MRI has greater diagnostic accuracy than CT, which is not surprising given the gated origin of the acquired images and the functional information that can be gleaned from MRI.

There are limitations to our study. The study was carried out in a quaternary referral center for PH, where patients were referred with suspected PH either from screening programs or due to the presence of symptoms. This group is at particularly high risk of having PAH; therefore it would be most appropriate to consider further noninvasive assessment in these patients. The CT pulmonary angiography used for evaluation of cardiac measurements was not cardiac-gated. However, CT performed for suspected PH is not routinely cardiac-gated and our study reflects the utility of CT that is typically performed in a routine clinical setting. In a recent report, Meune, *et al* proposed a score to stratify risk of PAH based on clinical tests in patients with SSc[41]. Selecting patients using such a risk stratification tool might be an option, especially in the low-risk population. However, our results show the value of MRI in a high-risk group.

Our results show that cardiac MRI had diagnostic accuracy similar to that of TG measurement, when this could be assessed using echocardiography; and it is superior to CT in assessing the severity of disease and diagnosing PAH in patients with CTD who are at high risk of having PAH. MRI can identify with a high degree of certainty patients likely to have PAH and may be of particular value in patients with suspected PAH who have poor-quality echocardiograms or in patients reluctant to have invasive investigation in establishing a positive diagnosis of PAH. In addition, cardiac MRI also offers the added advantage of predicting mortality in this subgroup of patients with CTD-PAH, and may be valuable in identifying patients for more aggressive therapy. Neither imaging test can confidently exclude PAH and right heart catheterization remains the definitive investigation to do this in patients with ongoing symptoms despite reassuring noninvasive investigations.

REFERENCES

1. Steen VD, Medsger TA. Changes in causes of death in systemic sclerosis, 1972-2002. Ann Rheum Dis 2007;66:940-4.
2. Wigley FM, Lima JA, Mayes M, McLain D, Chapin JL, Ward-Able C. The prevalence of undiagnosed pulmonary arterial hypertension in subjects with connective tissue disease at the secondary health care level of community-based rheumatologists (The UNCOVER Study). Arthritis Rheum 2005;52:2125-32.
3. Condliffe R, Kiely DG, Peacock AJ, Corris PA, Gibbs JS, Vrapi F, et al. Connective tissue disease-associated pulmonary arterial hypertension in the modern treatment era. Am J Respir Crit Care Med 2009;179:151-7.
4. Fisher MR, Mathai SC, Champion HC, Girgis RE, Housten-Harris T, Hummers L, et al. Clinical differences between idiopathic and scleroderma-related pulmonary hypertension. Arthritis Rheum 2006;54:3043-50.
5. Hurdman J, Condliffe R, Elliot CA, Davies C, Hill C, Wild JM, et al. Aspire Registry: Assessing the spectrum of pulmonary hypertension identified at a referral centre. Eur Respir J 2011 Sep 8 (E-pub ahead of print).
6. Ley S, Grunig E, Kiely DG, van Beek E, Wild J. Computed tomography and magnetic resonance imaging of pulmonary hypertension: Pulmonary vessels and right ventricle. J Magn Reson Imaging 2010;32:1313-24.
7. Alunni JP, Degano B, Arnaud C, Tetu L, Blot-Souletie N, Didier A, et al. Cardiac MRI in pulmonary artery hypertension: Correlations between morphological and functional parameters and invasive measurements. Eur Radiol 2010;20:1149-59.
8. Ley S, Mereles D, Puderbach M, Gruenig E, Schock H, Eichinger M, et al. Value of MR phase-contrast flow measurements for functional assessment of pulmonary arterial hypertension. Eur Radiol 2007;17:1892-7.

9. Dellegrottaglie S, Sanz J, Poon M, Viles-Gonzalez JF, Sulica R, Goyenechea M, et al. Pulmonary hypertension: Accuracy of detection with left ventricular septal-to-free wall curvature ratio measured at cardiac MR. Radiology 2007;243:63-9.
10. Roeleveld RJ, Marcus JT, Boonstra A, Postmus PE, Marques KM, Bronzwaer JG, et al. A comparison of noninvasive MRI-based methods of estimating pulmonary artery pressure in pulmonary hypertension. J Magn Reson Imaging 2005;22:67-72.
11. Elliot C, Kiely DG. Pulmonary hypertension: Diagnosis and treatment. Clin Med 2004;4:211-5.
12. Sharp GC, Irvin WS, Tan EM, Gould RG, Holman HR. Mixed connective tissue disease — An apparently distinct rheumatic disease syndrome associated with a specific antibody to an extractable nuclear antigen (ENA). Am J Med 1972;52:148-59.
13. Bohan A, Peter JB. Polymyositis and dermatomyositis (first of two parts). N Engl J Med 1975;292:344-7.
14. LeRoy EC, Black C, Fleischmajer R, Jablonska S, Krieg T, Medsger TA Jr, et al. Scleroderma (systemic sclerosis): Classification, subsets and pathogenesis. J Rheumatol 1988;15:202-5.
15. Tan RT, Kuzo R, Goodman LR, Siegel R, Haasler GB, Presberg KW. Utility of CT scan evaluation for predicting pulmonary hypertension in patients with parenchymal lung disease. Medical College of Wisconsin Lung Transplant Group. Chest 1998;113:1250-6.
16. Reid JH, Murchison JT. Acute right ventricular dilatation: A new helical CT sign of massive pulmonary embolism. Clin Radiol 1998;53:694-8.
17. Groves AM, Win T, Charman SC, Wisbey C, Pepke-Zaba J, Coulden RA. Semi-quantitative assessment of tricuspid regurgitation on contrast-enhanced multidetector CT. Clin Radiol 2004;59:715-9.
18. Bezante GP, Rollando D, Sessarego M, Panico N, Setti M, Filaci G, et al. Cardiac magnetic resonance imaging detects subclinical right ventricular impairment in systemic sclerosis. J Rheumatol 2007;34:2431-7.
19. Hagger D, Condliffe R, Woodhouse N, Elliot CA, Armstrong IJ, Davies C, et al. Ventricular mass index correlates with pulmonary artery pressure and predicts survival in suspected systemic sclerosis-associated pulmonary arterial hypertension. Rheumatology 2009;48:1137-42.
20. Kind T, Mauritz GJ, Marcus JT, van de Veerdonk M, Westerhof N, Vonk-Noordegraaf A. Right ventricular ejection fraction is better reflected by transverse rather than longitudinal wall motion in pulmonary hypertension. J Cardiovasc Magn Reson 2010;12:35.
21. Jardim C, Rochitte CE, Humbert M, Rubenfeld G, Jasinowodolinski D, Carvalho CR, et al. Pulmonary artery distensibility in pulmonary arterial hypertension: An MRI pilot study. Eur Respir J 2007;29:476-81.
22. Simonneau G, Robbins IM, Beghetti M, Channick RN, Delcroix M, Denton CP, et al. Updated clinical classification of pulmonary hypertension. J Am Coll Cardiol 2009;54 Suppl:S43-54.
23. Condliffe R, Radon M, Hurdman J, Davies C, Hill C, Akil M, et al. CT pulmonary angiography combined with echocardiography in suspected systemic sclerosis-associated pulmonary arterial hypertension. Rheumatology 2011;50:1480-6.
24. Denton CP, Cailes JB, Phillips GD, Wells AU, Black CM, Bois RM. Comparison of Doppler echocardiography and right heart catheterization to assess pulmonary hypertension in systemic sclerosis. Br J Rheumatol 1997;36:239-43.
25. Mukerjee D, St. George D, Knight C, Davar J, Wells AU, Du Bois RM, et al. Echocardiography and pulmonary function as screening tests for pulmonary arterial hypertension in systemic sclerosis. Rheumatology 2004;43:461-6.
26. Hsu VM, Moreyra AE, Wilson AC, Shinnar M, Shindler DM, Wilson JE, et al. Assessment of pulmonary arterial hypertension in patients with systemic sclerosis: Comparison of noninvasive tests with results of right-heart catheterization. J Rheumatol 2008;35:458-65.
27. Busteed S, Moots RJ, Thompson RN. Screening for pulmonary arterial hypertension in systemic sclerosis. Rheumatology 2004;43:1315-6; reply 6.
28. Hachulla E, de Groote P, Gressin V, Sibilia J, Diot E, Carpentier P, et al. The three-year incidence of pulmonary arterial hypertension associated with systemic sclerosis in a multicenter nationwide longitudinal study in France. Arthritis Rheum 2009;60:1831-9.
29. van Wolferen SA, Marcus JT, Boonstra A, Marques KM, Bronzwaer JG, Spreeuwenberg MD, et al. Prognostic value of right ventricular mass, volume, and function in idiopathic pulmonary arterial hypertension. Eur Heart J 2007;28:1250-7.
30. Saba TS, Foster J, Cockburn M, Cowan M, Peacock AJ. Ventricular mass index using magnetic resonance imaging accurately estimates pulmonary artery pressure. Eur Respir J 2002;20:1519-24.
31. Nijveldt R, Germans T, McCann GP, Beek AM, van Rossum AC. Semi-quantitative assessment of right ventricular function in comparison to a 3D volumetric approach: A cardiovascular magnetic resonance study. Eur Radiol 2008;18:2399-405.
32. Kahan A, Allanore Y. Primary myocardial involvement in systemic sclerosis. Rheumatology 2006;45 Suppl 4:iv14-7.
33. Bradlow WM, Assomull R, Kilner PJ, Gibbs JS, Sheppard MN, Mohiaddin RH. Understanding late gadolinium enhancement in pulmonary hypertension. Circ Cardiovasc Imaging 2010;3:501-3.
34. Tzelepis GE, Kelekis NL, Plastiras SC, Mitseas P, Economopoulos N, Kampolis C, et al. Pattern and distribution of myocardial fibrosis in systemic sclerosis: A delayed enhanced magnetic resonance imaging study. Arthritis Rheum 2007;56:3827-36.
35. Allanore Y, Meune C, Vonk MC, Airo P, Hachulla E, Caramaschi P, et al. Prevalence and factors associated with left ventricular dysfunction in the EULAR Scleroderma Trial and Research group (EUSTAR) database of patients with systemic sclerosis. Ann Rheum Dis 2010;69:218-21.
36. Kawut SM, Taichman DB, Archer-Chicko CL, Palevsky HI, Kimmel SE. Hemodynamics and survival in patients with pulmonary arterial hypertension related to systemic sclerosis. Chest 2003;123:344-50.
37. Gan CT, Lankhaar JW, Westerhof N, Marcus JT, Becker A, Twisk JW, et al. Noninvasively assessed pulmonary artery stiffness predicts mortality in pulmonary arterial hypertension. Chest 2007;132:1906-12.
38. Devaraj A, Wells AU, Meister MG, Corte TJ, Hansell DM. The effect of diffuse pulmonary fibrosis on the reliability of CT signs of pulmonary hypertension. Radiology 2008;249:1042-9.
39. Tunon J, Cordoba M, Rey M, Almeida P, Rabago R, Sanchez-Cascos A, et al. Assessment of chronic tricuspid regurgitation by colour Doppler echocardiography: A comparison with angiography in the catheterization room. Eur Heart J 1994;15:1074-84.
40. Revel MP, Faivre JB, Remy-Jardin M, Delannoy-Deken V, Duhamel A, Remy J. Pulmonary hypertension: ECG-gated 64-section CT angiographic evaluation of new functional parameters as diagnostic criteria. Radiology 2009;250:558-66.
41. Meune C, Avouac J, Airo P, Beretta L, Dieude P, Wahbi K, et al. Prediction of pulmonary hypertension related to systemic sclerosis by an index based on simple clinical observations. Arthritis Rheum 2011;63:2790-6.